Journal of Plankton Research, 2026, **48**, fbag065
https://doi.org/10.1093/plankt/fbag065
Original Article

Environmental forcing reshapes copepod functional diversity in the Northwest Atlantic

Niall McGinty[1,*], Andrew Irwin[2] and Catherine L. Johnson[3]

[1]Marine and Freshwater Institute, Fornubúðum 5, Hafnarfjörður, Iceland
[2]Dept. Mathematics & Statistics, Dalhousie University, Halifax, Canada
[3]Fisheries and Oceans, Bedford Institute of Oceanography, Bedford, Canada

*Corresponding author: nmcginty@dal.ca

Corresponding Editor: Hans Dam

ABSTRACT

Zooplankton are central to pelagic ecosystem functioning, mediating energy transfer and are sensitive indicators of climate-driven change. While shifts are well documented in zooplankton taxonomy and abundance, their implications for ecosystem functioning remain less clear. Functional trait approaches provide a mechanistic framework to link community composition with ecological processes by focusing on traits that govern feeding, growth, and energy transfer. We applied a trait-based analysis to long-term copepod communities at two time series sites on the northwest Atlantic shelf collected between 1999 and 2021 (HL2 and P5) to assess how environmental variability structures functional composition and diversity. Guided by biodiversity–ecosystem functioning theory, we hypothesized that environmental change would re-organize communities along dominant trait gradients, favour smaller and more metabolically active taxa under warming, and produce region-specific responses due to contrasting hydrographic conditions. There were declines in overall copepod biomass driven by the declining contributions of large lipid-rich copepods and increasing relative importance of smaller taxa with higher metabolic rates. Functional richness and dispersion generally tracked richness-based expectations, suggesting functional redundancy despite trends in trait composition. These results demonstrate that environmental variability is reshaping copepod functioning and highlight the value of trait-based approaches for understanding ecosystem responses to climate change.

KEYWORDS: copepods; traits; functional diversity; carbon; temperature; nutrients

INTRODUCTION

Zooplankton play a vital role in the ecosystem functioning of the pelagic system through both direct and indirect impacts on the bioavailability of nutrients and energy flow in an ecosystem (Hébert *et al.,* 2017). They are key indicators of climate-mediated changes in pelagic ecosystems, as evidenced by shifts in community structure (Steinberg *et al.,* 2015), abundance (Edwards *et al.,* 2021), and distribution (Beaugrand *et al.,* 2002). While taxonomic changes have occurred in zooplankton communities globally, much less is known about how these changes affect pelagic ecosystem functioning (Deschamps *et al.,* 2024). For example, shifts in the taxonomy could lead to changes in ecosystem functioning by altering the trophic transfer efficiency (Prowe *et al.,* 2019) or changes to the overall carbon biogeochemistry (Heneghan *et al.,* 2020) through changes in functional trait composition. Functional traits are characteristics of a species that determine their fitness in a particular ecosystem and provide information on their contribution to ecosystem functioning (Kiørboe, 2011; Hébert *et al.,* 2016). Functional trait-based approaches offer a powerful framework to mechanistically link community composition with ecosystem processes, biodiversity–ecosystem functioning relationships, and species responses to environmental change (Pomerleau *et al.,* 2015; Benedetti *et al.,* 2018).

Since the review by Litchman *et al.* (2013), which proposed that trait-based approaches are important for describing zooplankton communities, significant effort has been made to compile functional trait information for a range of zooplankton, especially copepods (e.g. Benedetti *et al.,* 2016; Brun *et al.,* 2017; Pata and Hunt, 2025). Over the last decade, trait-based studies have highlighted some of the regional and global variation in the zooplankton trait space. Body size has shown to be a key trait for copepods and appears to follow Bergmann's rule (Campbell *et al.,* 2021) where larger bodied species are more prevalent at colder temperatures (McGinty *et al.,* 2018; Becker *et al.,* 2024; Benedetti *et al.,* 2025). Other traits also display regional differences in their distribution with more ambush feeding taxa (Prowe *et al.,* 2019) and herbivores-omnivores in colder waters (Becker *et al.,* 2021; Benedetti *et al.,* 2023). Studies in the North Sea revealed a decoupling in the observed shifts in taxonomic composition and the ecosystem functioning of the zooplankton community (Djeghri *et al.,* 2023). Therefore, it is critical to examine time-series for changes in the trait

Received: September 15, 2025. **Revised:** July 24, 2026. **Accepted:** July 27, 2026

composition and functional diversity (FD) and not just changes in taxonomy.

However, limited trait harmonization, high trait plasticity, sparse long-term functional trait measurements, and scale-dependent ecological processes have collectively constrained our understanding of how zooplankton FD links to ecosystem functioning. Relationships between FD and ecosystem functioning may vary in direction and strength across different spatial scales (Gonzalez *et al.,* 2020). A broader range of traits may enhance complementary resource use within ecosystems, thereby increasing ecosystem production and functioning (*niche complementarity hypothesis*; McCann, 2000). Conversely, a system could be dominated by a few dominant species meaning production could decline or remain unchanged despite changes in trait richness (*mass-ratio hypothesis* Grime, 1998). Functional diversity is a multi-faceted concept where different indices may relate differently to shifts in taxonomy and provide indicators as to how ecosystem functioning might respond to these taxonomy changes. Emerging evidence from marine plankton communities suggests that ecosystem functioning may depend less on the total number of traits present and more on how traits are distributed among taxa. For example, whether species differ in body size, feeding strategy, or trophic role, influencing resource partitioning, trophic interactions, and carbon export efficiency (Brun *et al.,* 2019; Benedetti *et al.,* 2025). Functional redundancy can enhance ecosystem resilience by buffering against species loss, decoupling species richness from ecosystem functioning so that more species do not necessarily translate into greater functional output (Hooper *et al.,* 2005). Functional redundancy may buffer changes in species composition by maintaining dominant trait combinations linked to ecosystem functioning, consistent with the mass-ratio hypothesis (Benedetti *et al.,* 2025). Such patterns have started to be addressed on a global scale by Benedetti *et al.* (2025), yet they remain widely unexplored on local to regional scales.

Copepods are numerically dominant in the Northwest Atlantic, often comprising up to 80% of total zooplankton biomass in the area (Head *et al.,* 2003). Copepods not only serve as a primary energy pathway to higher trophic levels, including commercially important fish and marine mammals (Sameoto *et al.,* 1994; Sorochan *et al.,* 2019), but also play a pivotal role in the biological carbon pump both passively in the form of faecal pellets and actively through diel and seasonal migrations (Jónasdóttir *et al.,* 2015). Large copepod species belonging to the genus *Calanus* are ecologically important components of the ecosystem. These species deal with the short phytoplankton bloom duration by accumulating energy-rich lipids which allow individuals to diapause at depth (Record *et al.,* 2018). Spatial variation in the lipid content of these species can influence the available energy requirements for higher trophic levels (Helenius *et al.,* 2024). There have been significant changes in the spatial and temporal variability in zooplankton assemblages, driven by shifts in dominant water masses, phenological timing, and regional circulation patterns (Johnson *et al.,* 2011; Pepin *et al.,* 2015). Decreases in the abundance of some larger bodied copepods and gradual increases in smaller bodied copepods have been seen during warmer years. Continued shifts towards smaller organisms could lead to less suitable prey for higher trophic levels or a weaker contribution of copepods to the biological carbon pump (Becker *et al.,* 2024). These analyses largely focused on taxonomy and, as such, do not fully capture how observed community shifts influence ecosystem functioning. Different copepod species may fulfil similar or distinct ecological roles, and changes in taxonomic composition may not translate into changes in function, depending on trait redundancy within the community (Severo *et al.,* 2026).

Building on trait-based biodiversity–ecosystem functioning theory, we frame our expectations regarding how environmental variability reshapes copepod community trait composition, FD, and the ecosystem functions these traits support. First, under the mass-ratio hypothesis, ecosystem functioning is primarily driven by the traits of dominant taxa, such that shifts in community weighted mean traits (e.g. body size, feeding strategy) are expected to influence trophic transfer efficiency and carbon export. In this context, we expect increases in smaller-bodied, rapidly reproducing taxa to favour recycling pathways and microbial loop dominance, whereas larger, lipid-rich taxa should enhance carbon export efficiency. Second, functional redundancy may buffer ecosystem functioning against species turnover when taxa occupy similar regions of trait space. Thus, communities with constrained trait dispersion may maintain function despite changes in species composition. However, dependence on a limited number of dominant functional groups could increase vulnerability to their loss. Conversely, greater trait dispersion may indicate increased niche differentiation but reduced redundancy. We hypothesized that (Barton *et al.,* 2013) environmental forcing would drive coherent shifts in community-weighted trait composition along dominant size, trophic, and metabolic gradients, (Beaugrand *et al.,* 2002) these shifts would manifest as changes in overall FD reflecting trait filtering and reorganization rather than simple species turnover, and (Beaugrand *et al.,* 2003) regional oceanographic context would modulate the strength and direction of these responses. By integrating functional group composition, community-weighted traits, and multiple facets of FD, we aimed to resolve how bottom-up environmental controls propagate through zooplankton trait structure to influence trophic pathways, carbon export efficiency, and ecosystem functioning of the coastal ecosystems within the NW Atlantic Ocean.

METHODS

The Atlantic Zone Monitoring Programme (AZMP) is a long-term monitoring initiative designed to characterize the physical, chemical, and biological properties of the northwest Atlantic, with particular focus on the Canadian shelf ecosystems (Therriault *et al.,* 2002). Since 1999, the AZMP has provided an extensive time series of seasonal and monthly biological observations, including mesozooplankton, on cross-shelf transects and at fixed stations. We focus on two monitoring stations in the Bay of Fundy at Station Prince 5 (P5) and on the Scotian shelf Halifax 2 (HL2) which were sampled at regular monthly or semi-monthly intervals between 1999 and 2021 (Fig. 1). Both time series are situated at a similar latitude but with contrasting hydrographic regimes. This contrast allows us to examine how copepod functional traits and diversity respond to environmental variability

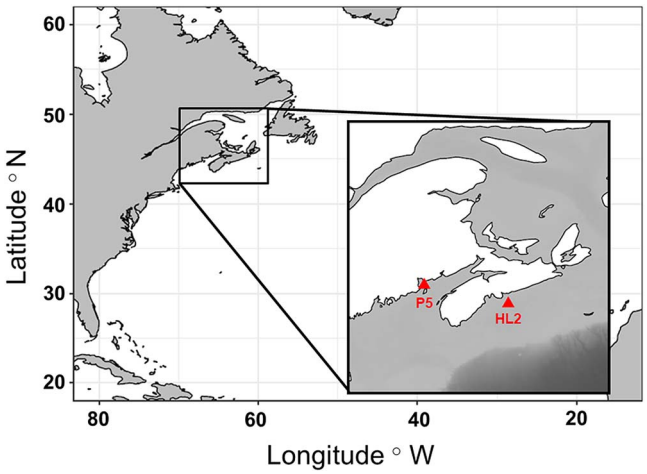

Fig. 1. A map displaying the position of the two fixed sampling stations in the bay of Fundy (P5) and on the central Scotian shelf (HL2).

across distinct ecosystem types, from a more stratified shelf system (HL2) to a highly productive, mixed coastal regime (P5), and to assess the extent to which functional reorganisation is consistent or context-dependent across these environments.

Zooplankton are collected using ring nets with a 0.75 m mouth opening and 202 μm mesh size which are towed vertically from 10 m above the bottom to the surface. Bottom depth is 149 m at HL2 and 100 m at P5. Samples are preserved in a 4% solution of buffered formaldehyde. Samples are analyzed using the AZMP protocol (Mitchell *et al.*, 2002). At the time of analysis, all organisms larger than 1 cm are separated out from the sample, identified, counted and weighed. The remainder of the sample is split, and half is used to estimate abundance and species composition in a subsample of a minimum of 200 organisms. An additional subsample is analyzed to identify, stage, and quantify at least 75–100 *Calanus* spp., or at least 150–200 *Calanus* spp. if several stages and/or all species were present. Copepods are identified to species level whenever possible, but some small, taxonomically similar copepods such as *Pseudocalanus* spp. are identified only to genus. Non-copepods are identified at either the species, genus, or higher taxonomic level depending on taxonomic group.

Copepod data

We focus on the copepod species collected by the AZMP due to their ecological importance within the ecosystem and their ubiquity within the samples, often comprising up to 80% of the total biomass. We restricted our selection to taxa that were collected at least once from both locations with 38 taxa being retained, 27 of which were identified to species level. Monthly time series of copepod abundance (number of individuals m^{-3}) between 1999 and 2021 were created. The total number of individuals was converted into total dry weight for individual taxa found in the trait database compiled by (Pata and Hunt, 2025). Missing species were filled using linear body length—dry weight relationships of available species (Supplementary Table 1). Genus only categories comprise largely copepodite stages of that group. Total body lengths of these groups are estimated by using the mean length of the copepodite stage V of the known species of that genus weighted by the abundance of each one (Supplementary Table 2). The total mass of a species within a sample can be found by multiplying the dry weights of each taxon by the total number of individuals. Of the 246 monthly values, there were 24 and 21 missing months at HL2 and P5 respectively. Estimates of missing values were imputed by Kalman smoothing which uses state-space time-series modelling and temporal autocorrelation structure using the R package *imputeTS* (Moritz and Bartz-Beielstein, 2017).The long-term trends were averaged across the 12 months to produce annual abundance estimates for each species while monthly climatologies were calculated from the same data.

Environmental data

At each station concurrent CTD casts are performed alongside the vertical net hauls. Water samples are selected at discrete depths within the upper 150 m for nutrients (nitrate, silicate and phosphate) and chlorophyll-*a* while temperature, salinity, and density are obtained from the sensors onboard the CTD. For salinity, nutrients, and temperature, average values of the upper 50 m are used as environmental covariates. Integrated chlorophyll-*a* collected at fixed depth in the upper 150 m is used as a proxy of total phytoplankton biomass (mg m^{-2}). Stratification is estimated by using the potential energy anomaly (PEA) where higher PEA equals strong stratification conditions and *vice versa*. Like the copepod data, missing values were imputed using Kalman smoothing. To focus on interannual variability rather than the dominant seasonal cycle, we calculated standardized monthly anomalies for each environmental variable relative to the long-term monthly climatology. For each calendar month, the long-term mean was subtracted from each observation and divided by the corresponding monthly standard deviation. Annual anomalies were then calculated as the mean of the standardized monthly anomalies within each year.

Functional diversity

We selected 12 functional traits that have been routinely used in zooplankton trait-based ecology and were compiled from several published databases. Trait types represent different ecological functions that include morphological (body size and myelination), behavioural (feeding mode and dietary preference) and life history (dormancy, spawning strategies), according to the framework of Litchman *et al.* (2013). Much of the categorical trait information were compiled from the trait table compiled by Benedetti *et al.* (2025). Information on body size, dry weights (including carbon and nitrogen) and metabolic rates (respiration and excretion) are derived from the trait database compiled by Pata and Hunt (2025). Respiration and ammonium excretion rates were first temperature-corrected from their reference measurement temperature (15°C) to 7.5°C, corresponding to the mean (0-50 m) temperature of the study region, using a Q_{10} formulation ($Q_{10} = 2.0$ for respiration and 2.5 for excretion) to obtain weight specific metabolic rates dividing by species-specific individual carbon mass. Allometric scaling was used to estimate missing species trait information (Supplementary Table 1). Stoichiometric ratio

of carbon:nitrogen (C:N) was obtained from the individual dry carbon and nitrogen weights.

To determine the functional trait space, we used a combination of individual categorical and continuous variables or fuzzy-coded traits. These include both feeding mode and dietary strategy where more than one category could be applied to an individual taxon (e.g. Benedetti *et al.,* 2023). Due to the high correlation between scaled size and weight variables, only the carbon dry weight was used as the main body size trait. The trait dissimilarity between species is calculated using *gawdis* to calculate the gower index which allows for the categorisation of fuzzy-traits.

A principal coordinate analysis (PCoA) was performed on the dissimilarity matrix to create a multidimensional functional trait space for the copepod community. The PCoA axes are used to determine the functional trait space of the copepods where closely oriented spaces are more likely to share a similar suite of functional traits—(Mouillot *et al.,* 2021). To evaluate the correct number of axes used for calculating trait similarity we use the area under the curve (AUC) for co-ranking matrices. The selected axes k were then used to cluster taxa based on shared traits by calculating the Euclidean distance and the silhouette method to find the correct number of clusters. The clustered taxa represent groups with a shared trait profile and are known as functional groups (FG). The total biomass within each functional group is found by summing the species within each functional trait category at both P5 and HL2. The relative contribution of each functional group to the total biomass is shown for each year and month at both locations.

The PCoA represents a scaled representation of the multidimensional functional trait space for the entire dataset. Changes in the annual functional trait space were calculated by finding the annual community weighted means (CWM.Axis) for each PcoA axis *k* and year *y.* The abundance *a* of all species *s* present for each year *y* are multiplied by their PcoA axis score *p,* divided by the abundance *a* of all species *s* present for each year. Distances between each CWM year can be used to indicate the level of similarity in the functional trait space between years with larger distances indicating years with a greater change in trait functioning within the copepod community at P5 and HL2.

$$CWM.Axis_{yk} = \sum_{i=1}^{s} a_{iy}p_{ik} \Big/ \sum_{i=1}^{s} a_{iy}$$

A single combined PCoA trait space is generated for taxa present at both P5 and HL2. The FD indices are calculated by using the same PCoA scores and the annual time series abundances of taxa at each location. We calculate annual indices for functional evenness (FEve—How even traits are distributed across community), functional divergence (FDiv—Higher values suggest species with trait extremes dominate a community), functional dispersion (FDis—higher values suggest species are more different from another in a community) and functional Richness (FRic—Higher values suggest more of the trait space is occupied by species in a community). For continuous variables the annual community weighted mean (CWM) is calculated while for fuzzy coded variables such as feeding and dietary strategy the annual percentage of each trait is calculated. Since FRic is closely coupled with the overall species richness we calculate a standardized FRic (ses.FRic). We randomize the matrix adopting the independent swap algorithm which controls for year richness and species frequencies but randomizes taxa among years ($n = 999$). Ses.FRic is scaled such that values greater than 2 standard deviations indicate a significant change in functional richness where positive values indicate trait divergence while negative values indicate trait convergence (Götzenberger *et al.,* 2012). Functional redundancy was not quantified directly but inferred from patterns in FD indices. Low deviations in ses.FRic and constrained functional dispersion were interpreted as indicative of high functional redundancy, where multiple species share similar trait combinations.

Linking functional dynamics with the local environment

The CWM.Axes represent the dominant multivariate functional group patterns in each community. We used a redundancy analysis (RDA) to relate the matrix of annual CWM.Axis scores to our set of standardized environmental anomaly variables allowing us to identify the major environmental gradients explaining variation in functional composition. Statistical significance of the overall RDA model, individual axes, and terms was assessed using permutation tests, and environmental variables that were significant or near significant (< 0.2) contributors were retained for further modelling. These selected predictors were incorporated into generalized additive models (GAMs) to quantify potentially nonlinear relationships between environmental anomalies and each CWM axis, providing a more detailed characterization of trait–environment responses through time. Smooth terms were estimated using thin-plate regression splines, and the optimal number of smooth terms were determined using shrinkage selection allowing non-informative smoothers to be penalized towards zero and effectively excluded from the final model. To complement this trait-space analysis, we examined annual patterns in traditional FD indices and CWM of traits by correlating each index with corresponding yearly environmental anomalies. We constructed correlation-based association networks (Pearson's product–moment correlation) using *ggraph*, where nodes represented traits and environmental variables and edges represented significant positive or negative correlations. These networks allowed visualization of co-varying indices and environmental drivers, helping to identify potential mechanistic links and dominant controls shaping long-term functional dynamics.

These association networks were used to identify the FD indices and CWM that most strongly associated with environmental variability. In both time-series the CWM of C:N ratio correlated strongly ($r > \pm 0.9$) with the CWM of myelination, ambush, cruise and current feeding strategies and the omnivore-herbivore trophic level group and as a result were removed prior to constructing the association networks. Only significant correlations ($P < 0.05$) were represented in the networks. These networks provided insight into whether long-term functional change was driven primarily by shifts in dominant traits, trait dispersion, or broader changes in functional structure.

RESULTS

A total of 38 taxa were classed into four FG based on the hierarchical clustering of the first four PCoA axes (Fig. 2). The highest level of the dendrogram divided species based on the presence of Myelination (FG B and C) and non-myelination (FG A and D). Subsequent grouping divides FG based on reproduction mode and could be defined mainly by body sizes of individual taxa within the group, the different feeding modes and dietary strategies. FG A: Small sac-spawning current feeding omnivores consists of 5 taxa with a mean weight of 2.2 ug C individual^{-1}. Taxa largely come from the *Clausocalanidae* and the *Temoridae* families that are mainly current feeding omnivores. FG B: Broad sized Current feeding omnivore-herbivore consists of 10 taxa with a mean weight of 350 ug C individual^{-1}.While there is a broad range in carbon weights individual^{-1} across the groups representatives, smaller sized taxa make up less than 5% of the biomass at both locations. Taxa are almost exclusively current feeding species belonging to the *Calaninidae* and *Paracalanidae* families with just over half of the species undergoing dormancy. FG C: Small particle and mixed feeding detritivore-omnivore consists of 10 taxa and are comprised of species from the orders Cyclopoida and Harpacticoida which have the smallest mean weight of 0.22ug C individual^{-1}. These taxa are all sac-spawners and non-myelinated and are the only to include species largely associated with sinking particle feeding and have feeding appendages adapted to scraping detritus and microbial biofilms. FG D: Medium broadcast omnivores consist of 13 taxa with a mean carbon weight of 22ug C individual^{-1}. This group is also varied in their approach to dormancy and DVM and feeding strategy with similar numbers displaying the three trait categories found in each.

FG B remained the dominant functional group throughout the study period, accounting for the majority of copepod biomass at both HL2 and P5 (Fig. 3A, B). At HL2, all four functional groups exhibited significant directional changes in their relative biomass contributions between 1999 and 2020. At P5, trajectories initially differed from those at HL2 but after ~ 2010, with both stations showing declining contributions of FG B and increasing contributions of FG C and FG D. At HL2, the relative biomass contribution of FG B declined from ~90% to below 70% ($R^2 = 0.45$, $P < 0.001$), while at P5 it declined from ~95% to as low as 45% after 2010 ($R^2 = 0.39$, $P < 0.001$). Over the same period, FG D increased from ~10% to over 25% at HL2 ($R^2 = 0.48$, $P < 0.001$) and from less than 10% to as much as 45% at P5 ($R^2 = 0.34$, $P < 0.001$). FG C contributed less than 1% of relative biomass at both stations in 1999 but increased significantly to more than 5% at HL2 ($R^2 = 0.39$, $P = 0.001$) and ~4% at P5 after 2010 ($R^2 = 0.19$, $P = 0.024$). FG A remained a minor component (<5% of biomass), increasing slightly at HL2 ($R^2 = 0.15$, $P = 0.04$) but showing no significant temporal trend at P5.

There were no significant differences observed in the mean integrated chlorophyll-*a* at both locations (Station effect: $F = 0.82$, $P = 0.31$; Fig. 3C, D). Chlorophyll-*a* declined significantly at both stations, although the trend was stronger and more consistent at P5 ($F_{1,20} = 31.44$, $R^2 = 0.59$, $P < 0.001$) than at HL2 ($F_{1,20} = 4.68$, $R^2 = 0.15$, $P = 0.04$). In contrast, mean copepod dry-weight biomass was ~13-fold greater at HL2 (16 g m^{-3} +/− 5.7) than at P5 (1.2 g m^{-3} +/− 0.67) (Station effect: $F = 144$, $P < 0.001$; Fig. 3E, F). Total biomass declined significantly at HL2 ($F_{1,20} = 5.84$, $R^2 = 0.19$, $P = 0.02$), while P5 exhibited a steady decline after 2010 ($F_{1,20} = 5.18$, $R^2 = 0.22$, $P = 0.03$). Despite long-term declines in both, annual copepod biomass was only weakly and non-significantly related to integrated chlorophyll-*a* biomass at either station.

The multidimensional trait space of the 38 copepods is defined by the first two PCoA axes. The plot displays the relatedness between the species and the four FG shown in Fig. 2 and the first two axes explain 39% of the variation in the trait data (Fig. 4A). Many of traits were represented along the PCoA axis 1 represent a size-trophic feeding gradient where negative values represented species that were larger, current feeding omnivore-herbivores that were more likely to undergo diapause while positive values represented smaller taxa that were detritivore-omnivores or particle feeders but also included a mixed cruise or ambush feeding strategy (Fig. 4B). The PCoA axis 2 separates two FG with taxa of approximately equal size and represents separation of diapause strategies and cruise-feeding omnivores from ambush-feeders. The CWM.Axes for both P5 (red line) and HL2 (green line) are shown within the trait space (Fig. 4A) and expanded to show the annual progression within each time series. Changes in both time series are strongly associated with PCoA axis 1. For HL2, the CWM for each year is shifted more towards negative values close to FG B. Initially the time series shifts more towards FG B and negative values until 2008 before turning slightly less negative in the latter half of the time series towards FG C and FG D (Fig. 4C). At P5 we see similar early time series shifts towards negative values moving towards FG B before a post 2010 shift back toward slightly negative values (Fig. 4D). In contrast with HL2 the later years do shift beyond 1999 to more positive values but are more in-line with the initial PCoA axis 1 position.

The RDA finds that 46% of the variability in CWM at HL2 and 65% of the variation at P5. There are more balanced gradients across RDA1 and RDA2 at HL2 while a single strong gradient dominates at P5. At both locations opposing gradients in sea temperature and chlorophyll-*a* versus nutrients are the most dominant environmental patterns with the first two RDA axes. Only RDA 1 was significant at both locations. At HL2 the most significant terms were chlorophyll-*a*, phosphate, silicate and sea temperature while at P5 chlorophyll-*a*, nitrate, phosphate and sea temperature were the most significant. These variables were used to model the first two CWM.Axes against environmental anomalies using a GAM approach. Significant negative relationships were found between silicate and nitrate for CWM.Axis1 at both HL2 and P5 while at P5 sea temperature is also positively associated with CWM.Axis2 (Fig. 5). For CWM.Axis2 significant positive relationships with phosphate are found at both HL2 and P5 while at HL2 a negative relationship with sea temperature is also found (Fig. 5). Both the RDA and GAMs were analysed for temporal autocorrelation in the residuals, but none were found at either HL2 or P5.

Environmental correlations with functional indices differed markedly between HL2 and P5. At HL2, nutrient anomalies were positively associated with CWM C:N and negatively

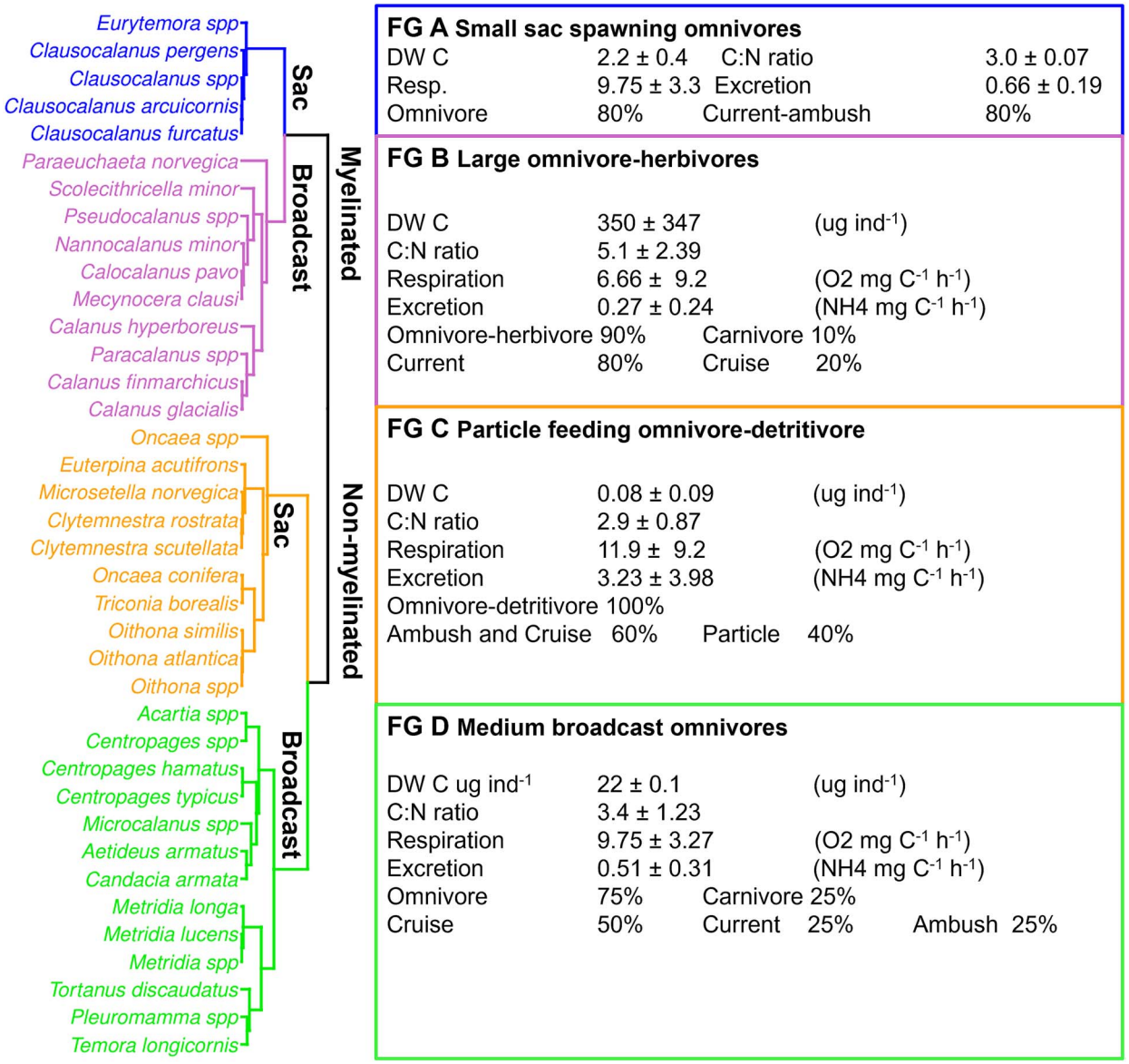

Fig. 2. A cluster dendrogram of the four functional groups based on the Gower dissimilarity using the PCoA axes. Species are coloured based on their association with each of the four FG. The dendrogram is divided broadly between predominantly broadcast spawning (FG) and sac spawning species (FG) and presence of myelination (FG). The mean ± sd the continuous traits and, percentage occurrence of each fuzzy coded traits within each FG is shown on the right.

associated with FDis. CWM C:N and the CWM of broadcast spawners also decreased over time while the FDis and the CWM of respiration increased. Temperature was not linked to changes in FDis but was negatively associated with the CWM of C:N and the dry weight of carbon and a positively association with both weight specific metabolic rates (Fig. 6A). There are fewer associations at P5 between environmental anomalies and traits, however those that are shared display the same direction (e.g. nitrate and FDis, temperature and CWM excretion). Temperature is more central at P5, which is positively linked to FDis, while silicate is positively linked here to the CWM of carbon dry weight (Fig. 6B). The ses.Fric is largely stable across both time series with much of the variation within expected variation although there are 2 years in 2006–2007 which show significant overdispersion at P5. FDis emerged as the most informative FD index in our analysis. We further tested how annual changes in species richness ($\Delta SR = SR_{t+1} — SR_t$) respond to annual changes in FDis ($\Delta FDis = FDis_{t+1} — FDis_t$) and found a weak correlation between both variables ($r = -0.6, P = 0.73$). Annual time series of each FD plots and CWM of continuous traits are shown in (Supplementary Fig. 1). Both time-series show that the CWM C:N ratio is negatively associated with the CWM of ambush and cruise feeding copepods ($r > -0.85$) and negatively associated with current feeding ($r > 0.88$) pointing to decreases of the community C:N ratios and prevalence of current feeding. Similarly, the herbivore dietary strategy is positively associated

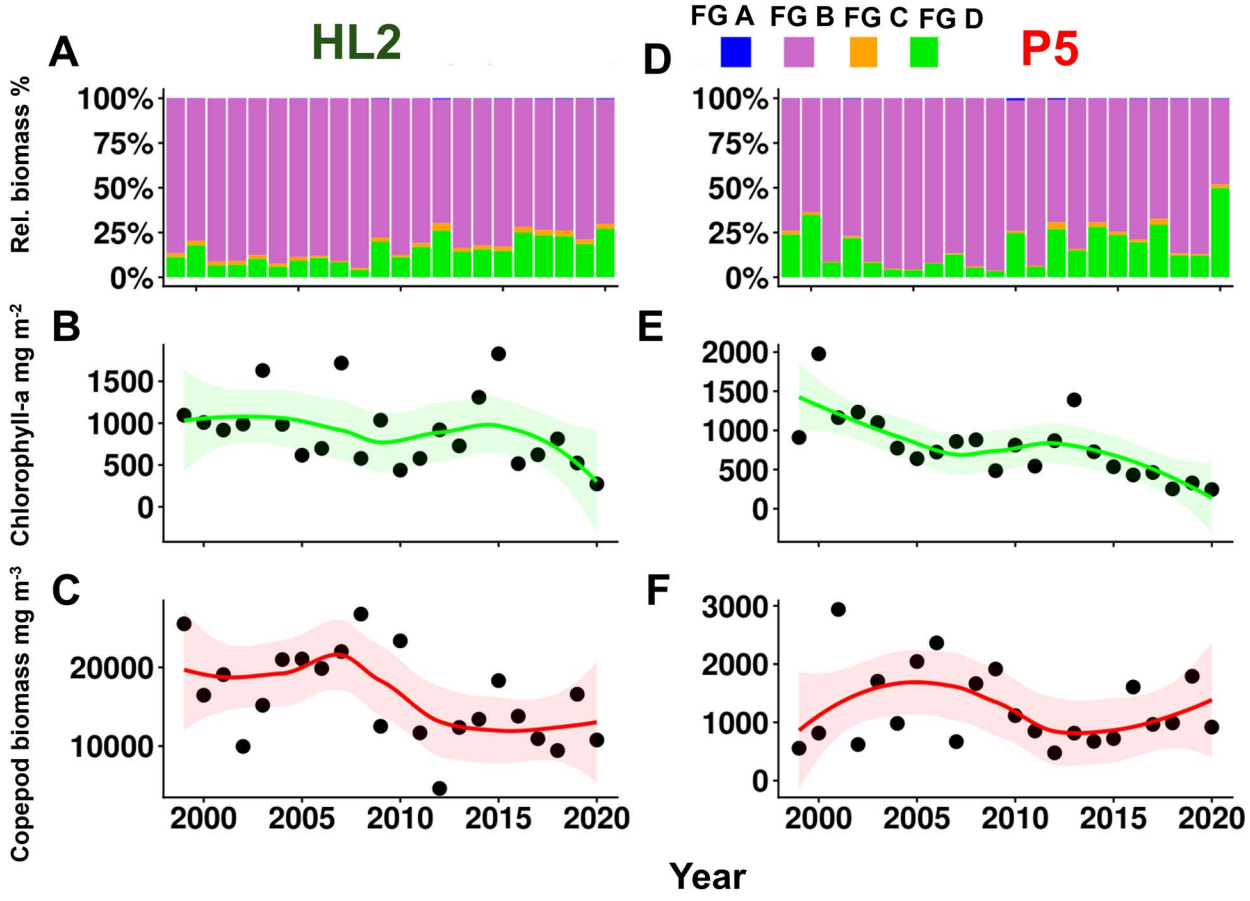

Fig. 3. Changes in the total percentage contribution for each of the four functional groups (A–D). Changes in the annual percentage contribution are shown for HL2 (A) and P5 (D). The total annual integrated chlorophyll-a (mg m^{-2}) biomass for HL2 (B) and P5 (E) and total annual copepod biomass in mg m^{-3} for HL2 (C) and P5 (F) are also shown.

with the CWM C:N ratios ($r > 0.86$) pointing to an overall decrease over time. Annual time series of each fuzzy feeding and dietary strategy are shown in (Supplementary Fig. 2).

DISCUSSION

The application of functional trait analysis to understand the dynamics of zooplankton communities represents a pivotal step towards linking ecosystem processes to broader environmental and climatic changes. We characterized the functioning of the copepod community structure at two long standing time series on the central Scotian shelf (HL2) and in the Bay of Fundy (P5). Our study revealed a coherent regional redistribution of biomass among functional groups, although the timing and magnitude of responses differed between systems. The core functional structure was dominated by FG B, there were clear indications that shifts in environment (i.e. nutrient decreases and temperature increases) favoured smaller sized taxa with higher metabolic rates (Figs 3 and 4). In addition to these common patterns, clear regional contrasts emerged. At both HL2 and P5, nutrient anomalies were strongly aligned with interannual shifts along the primary CWM axes, indicating that interannual changes in resource availability re-organized communities along dominant trait gradients rather than simply altering taxonomic composition (Fig. 5, Djeghri *et al.*, 2023). Nutrient availability appears to be a stronger predictor than phytoplankton biomass for changes in FG composition and overall biomass (Fig. 6). The gradual declines in copepod biomass and gradual redistribution among dominant functional groups at HL2 indicate tighter coupling between resource variability and copepod community structure on the Scotian Shelf, while at P5 there were delayed reductions in biomass and delayed changes in functional group redistribution, suggesting similar ecosystem restructuring that manifested more slowly in the Bay of Fundy.

Changes in environmental conditions post-2010

The contrasting responses between HL2 and P5 likely reflect broader regional oceanographic changes that intensified across the Northwest Atlantic after ~2010 (Meyer-Gutbrod *et al.*, 2021). This period has been associated with a major reorganization of Gulf of Maine and Scotian Shelf hydrography, including increased influence of Warm Slope Water, rapid regional warming, altered stratification, and reduced nutrient inventories (Pershing *et al.*, 2015; Record *et al.*, 2019; Lehmann *et al.*, 2023; Casault *et al.*, 2024). HL2 represents a more advective outer shelf environment strongly coupled to basin-scale circulation and slope water inflows, where these oceanographic shifts likely reduced the persistence of large oceanic calanoids and favored smaller, faster-growing taxa associated with warmer

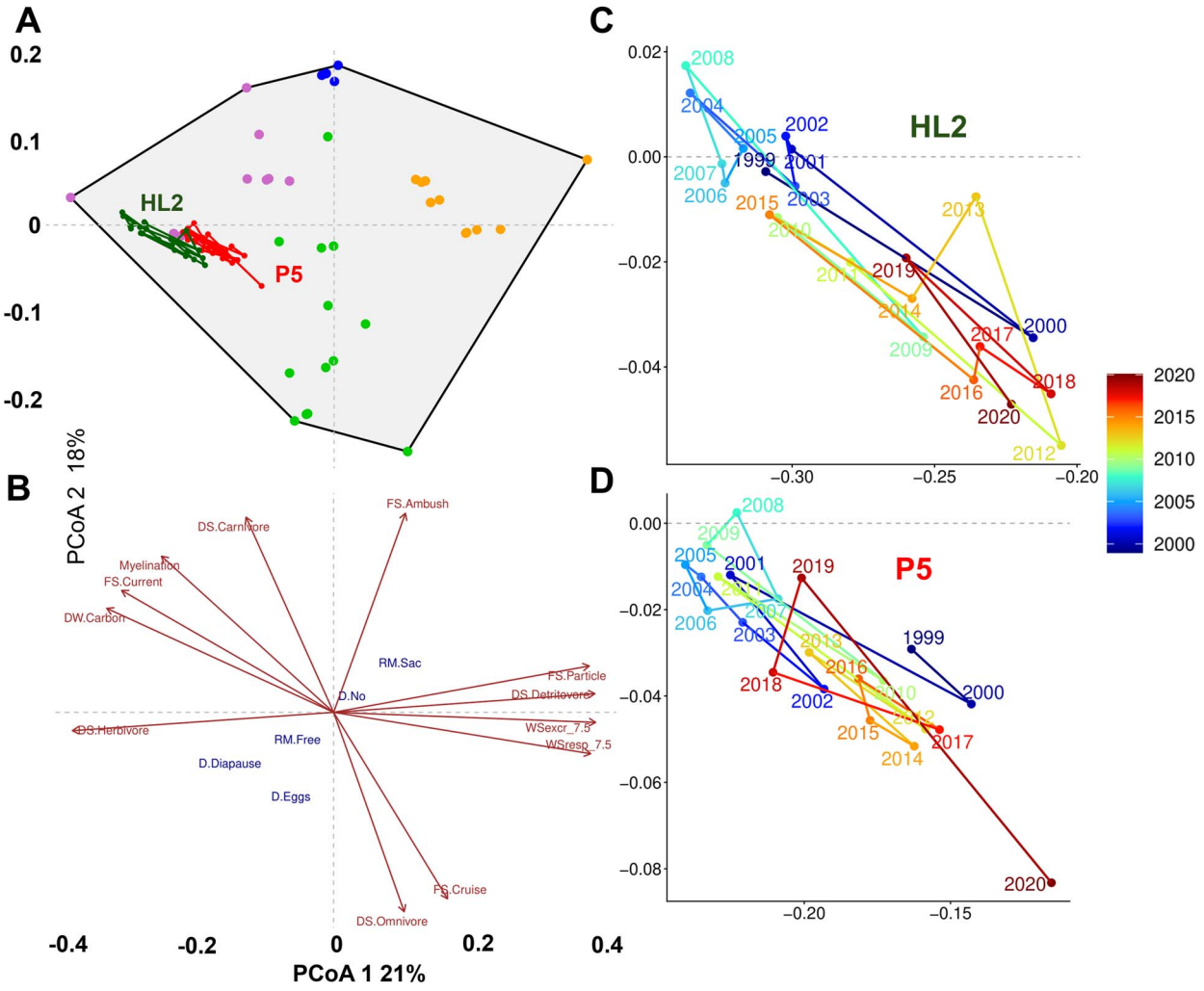

Fig. 4. PCoA ordination used to define the functional trait space. (A) The 38 copepod taxa found in both areas (colour following trait grouping in Fig. 2), bounded by a grey polygon to show the full trait space, and the community weighted mean (CWM) for each year at both Halifax line 2 (HL2, green) and Prince 5 (P5, red). The centroid is calculated by weighting PCoA values for each species by their annual abundance between 1999 and 2020. (B) Projections of the continuous and fuzzy (red) and categorical (blue) traits on to the PCoA axes. The trajectory of CWM shown in a is enlarged to show year to year changes for HL2 (C) and P5 (D). Points and lines are coloured to indicate years.

and more recycled production pathways. At HL2, nutrient anomalies, particularly nitrate and silicate, showed strong negative trends through time. This coincided with increases in functional dispersion (FDis), declining CWM body size and C:N ratios, and increasing weight-specific metabolic rates, indicating an increase in the relative importance of different FG rather than simple taxonomic turnover (Djeghri *et al.*, 2023; Pata *et al.*, 2025). These patterns are consistent with broader regional observations of post-2010 zooplankton reorganization in the Gulf of Maine, where declines in large lipid-rich *Calanus finmarchicus* were accompanied by increases in smaller copepod taxa, greater mesozooplankton diversity and a decline in total biomass under warmer conditions (Pershing *et al.*, 2021; Runge *et al.*, 2025). In contrast, P5 is embedded within the highly mixed Bay of Fundy system, where tidal mixing partially buffers stratification and nutrient depletion, and where environmental variability is more episodic and strongly linked to interannual fluctuations in Gulf of Maine inflows and regional warming events (Greene *et al.*, 2013; Pershing *et al.*, 2015). Although both systems exhibited similar environmental–trait relationships, the magnitude and persistence of functional restructuring were therefore substantially greater at HL2, suggesting that outer shelf copepod communities may be more sensitive to long-term hydrographic and nutrient-driven ecosystem change than tidally mixed coastal systems (Ji *et al.*, 2022; Runge *et al.*, 2025).

Links between functional groups, biomass and environmental anomalies

The total copepod biomass was on average substantially higher at HL2 than at P5. However, declines in FG B at HL2 coincided with reductions in total biomass and increasing FDis, suggesting that biomass was redistributed across a wider range of trait combinations rather than maintained within dominant large-bodied taxa. This pattern supports the mass-ratio hypothesis, whereby ecosystem functioning is disproportionately driven by the traits of dominant taxa rather than overall richness

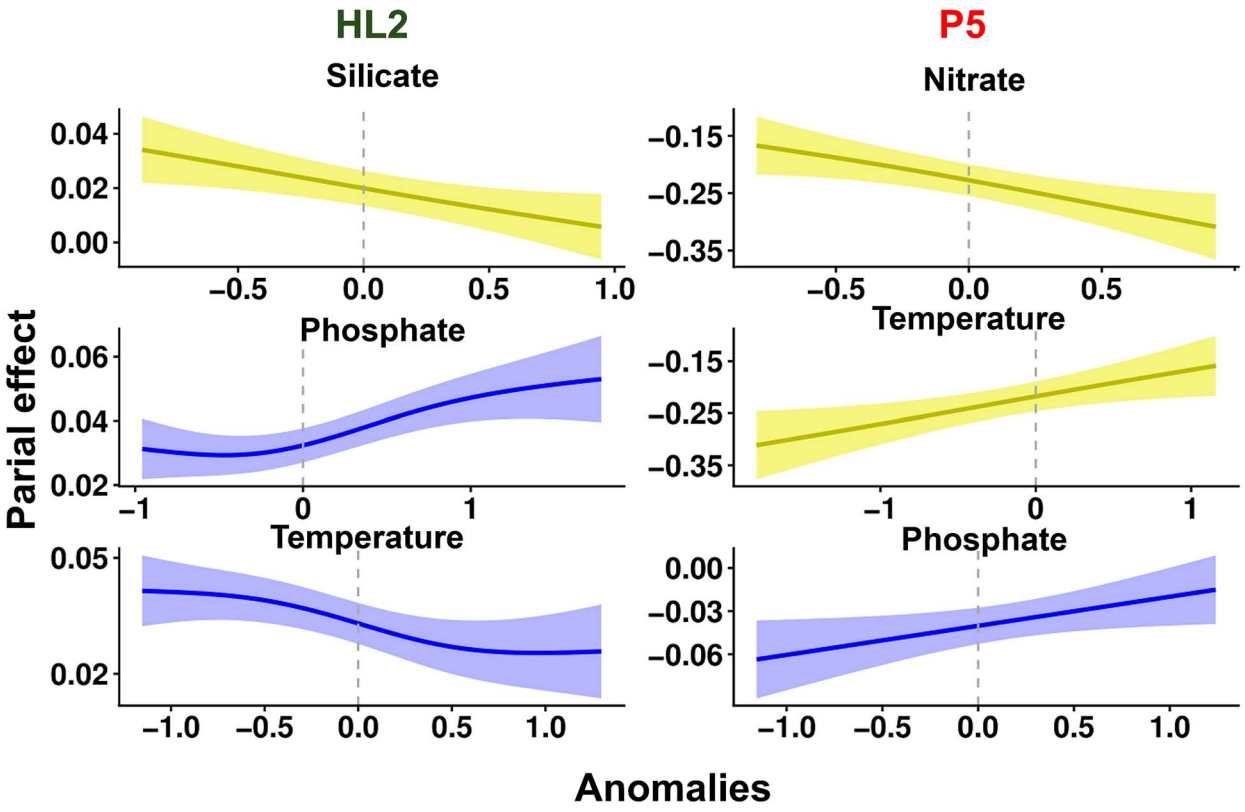

Fig. 5. The partial effect smoothers of the generalized additive models (gams) modelling the CWM axis 1 (yellow line and shaded 95% CI) and CWM axis 2 (blue line and shaded 95% CI) against the environmental anomalies of HL2 (left column) and P5 (right column). The environmental anomalies shown are named to the left of each panel figure.

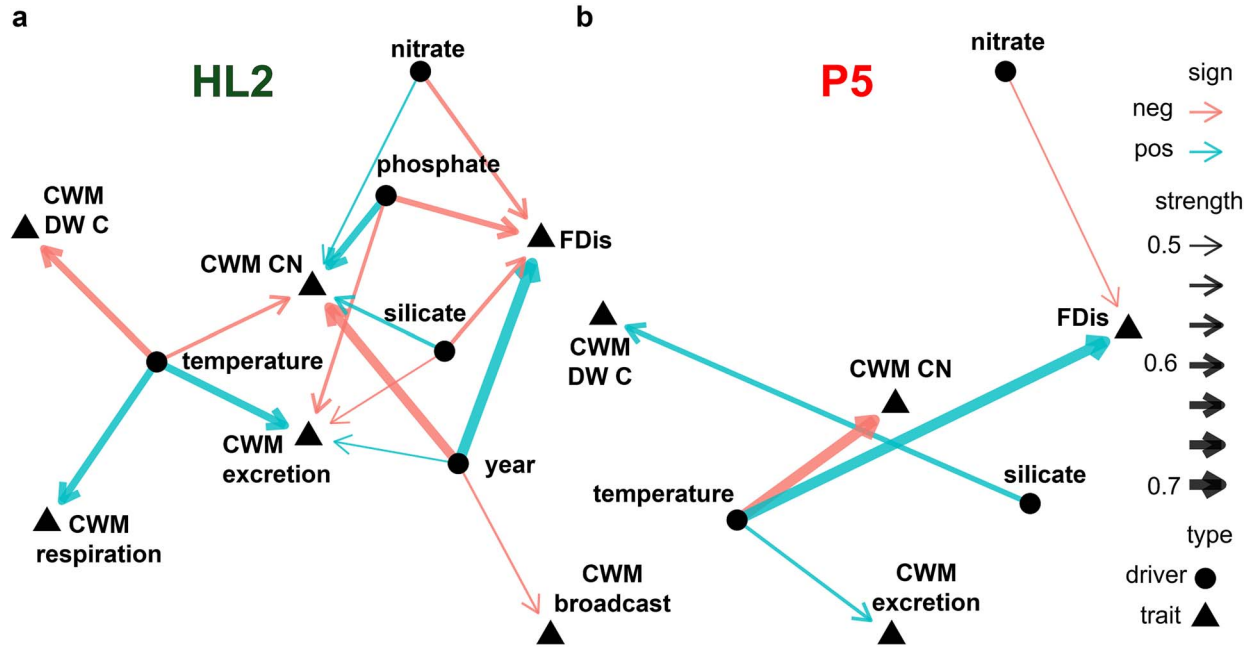

Fig. 6. The correlative relationship between environmental drivers (circle) and functional indices (triangle) at both HL2 (A) and P5 (B) when $P < 0.05$. The absolute strength is scaled by the thickness of the arrow where thicker lines signify stronger associations while colour indicates positive (blue) and negative (red) relationships.

or diversity (Benedetti *et al.*, 2025). In these systems, the large, myelinated lipid-rich *Calanus* complex tends to dominate (Brandão *et al.*, 2021) and contributes substantially to trophic transfer efficiency and carbon export through high biomass, elevated C:N ratios, and production of large fast-sinking fecal pellets (Melle *et al.*, 2015; Steinberg and Landry, 2017). The

observed decline in CWM body size and C:N ratio, together with increasing metabolic rates and FDis, is consistent with a reduced dominance of the large-bodied, lipid-rich FG B and an increased relative contribution of smaller functional groups exhibiting higher mass-specific metabolic rates and broader trophic strategies. (Kiørboe, 2011; Prowe *et al.,* 2019; Benedetti *et al.,* 2025).

The relationships between copepod functional structure and environmental variability differed substantially between HL2 and P5, highlighting the importance of regional hydrographic context in shaping ecosystem responses. While both systems exhibited interannual variability in community weighted mean (CWM) traits and functional indices, long-term directional change was more pronounced at HL2 on the Scotian Shelf than at the tidally mixed Bay of Fundy station P5. This contrast likely reflects differences in both oceanographic forcing and the underlying composition of dominant copepod assemblages (Head and Pepin, 2010; Johnson *et al.,* 2011; Record *et al.,* 2019). FG B remained the dominant contributor to copepod biomass throughout the time series at both HL2 and P5, although its relative biomass declined significantly at HL2 alongside increases in all other functional groups. The species composition within FG B did not shift substantially through time within either time-series, although the dominant taxa differed between them. At P5, FG B was largely represented by *C. finmarchicus*, which may initially have buffered declines in total FG B biomass. However, the eventual post-2010 reductions in FG B and concurrent increases in FG C and D suggest that this resistance weakened over time as warming and changing Gulf of Maine inflows increasingly altered Bay of Fundy ecosystem structure (Dullaert *et al.,* 2026). At HL2, biomass was shared more evenly among the different congeners of *Calanus spp*. which have known differences in their niches, phenologies, and advective sources (Freer *et al.,* 2022; Supplementary Fig. 3). Shifts in hydrographic forcing and nutrient supply at HL2 may have disproportionately altered the balance among these co-occurring large calanoids, contributing to the marked decline, whereas the more stable dominance of *C. finmarchicus* at P5 likely buffered comparable biomass losses.

While reproduction mode and myelination formed distinct FG similar to groups defined more broadly (Fig. 2; Benedetti *et al.,* 2023), myelinated species are more likely to be broadcast spawning omnivores-herbivores (Becker *et al.,* 2021) due to the role of myelination in predator avoidance and lipid accumulation (Lenz, 2012). Here we see that the CWM of these traits covaries quite strongly and decrease over time suggesting that the decline of large lipid-rich calanoid taxa simultaneously reduced multiple linked life-history and behavioural strategies, rather than independently restructuring each trait dimension (Benedetti *et al.,* 2025). We see also that the observed shift from current-feeding to cruise- and ambush-feeding strategies suggests increasing reliance on motile prey and regenerated production pathways rather than direct exploitation of large bloom-forming phytoplankton (Castellani *et al.,* 2005; Supplementary Fig. 2). Current feeders are typically linked to efficient exploitation of spring diatom blooms and enhanced vertical carbon export, whereas ambush and cruise feeders are more closely associated with microbial-loop and recycling-dominated food webs (Kiørboe, 2011; Prowe *et al.,* 2019). The strong correlation between feeding strategy composition and the CWM C:N ratio suggests that changes in trophic functioning and carbon cycling were tightly coupled to shifts in dominant feeding behaviours rather than simply body size alone (Heneghan *et al.,* 2020). The combined decline in total copepod biomass at HL2, coupled with a steady decline of FG B type taxa toward smaller, varied diet FG suggests not only a reduction in overall secondary production but a potential re-organisation of energy flow. Increases in FDis and a reduction in FG B dominance and an increase in the FG importance which represent a wider range of trait combinations, rather than an increase in total production, and are consistent with a shift away from a *Calanus*-dominated functional structure (Dullaert *et al.,* 2026). Previous trait-based studies suggest that chlorophyll or productivity gradients primarily enhance copepod biomass and herbivorous trophic pathways, whereas nutrient and hydrographic gradients more strongly structure functional composition, trophic organisation and ecosystem functioning (Nutrient availability influences more than just phytoplankton biomass but also their size structure, taxonomic composition, bloom phenology, and trophic pathways, which ultimately determine copepod functional composition Tang *et al.,* 2022; Huggett *et al.,* 2023; Severo *et al.,* 2026). Despite significant declines in chlorophyll-a at both stations, particularly at P5, these changes were not directly coupled to declines in total copepod biomass. This apparent decoupling suggests that copepod community structure may respond more strongly to changes in phytoplankton composition, bloom timing, and trophic pathway structure than to bulk phytoplankton biomass alone (Djeghri *et al.,* 2023).

Functional traits and ecosystem functioning

Our results do not indicate a complete replacement of FG B by other FG, but rather a redistribution of relative biomass among them (Fig. 4). FG D, which is the second most important FG and is composed of smaller omnivorous taxa such as *Acartia*, *Metridia*, and *Centropages*, increases over time while FG B declines. These taxa are associated with higher metabolic rates, broader diets, and greater coupling to regenerated production pathways (Møller *et al.,* 2007; Saba *et al.,* 2009). While the relative biomass of FG C is small, species such as *Oithona* spp. that comprise this FG are significantly underestimated by traditional net sampling with >200 μm mesh (Gallienne and Robins, 2001; Dahms *et al.,* 2015). The increases in both FG C and D suggest a retention of organic matter in the upper water column leading to increased microbial loop coupling, and reduced export efficiency (Pomeroy *et al.,* 2007; Turner, 2015). Environmental conditions favouring this redistribution likely include reduced nutrient inventories, warmer surface waters, enhanced stratification, and weaker bloom intensity, all of which are expected to promote smaller phytoplankton and more microbial-loop dominated food webs (Morán *et al.,* 2017).

The observed negative relationship between temperature and copepod body size is consistent with broader evidence that warming promotes smaller-bodied, faster-growing taxa with higher metabolic demands (Campbell *et al.,* 2021; Tang *et al.,* 2022). Increases in mass-specific respiration and excretion rates

further support this interpretation. However, these responses likely reflect both direct physiological constraints and indirect ecological mechanisms, including altered phytoplankton size structure, phenological mismatch, and changing predation pressure (Wiebe *et al.,* 2022; Pershing and Kemberling, 2024). Such mechanisms appear particularly important in the Gulf of Maine–Bay of Fundy region, where recent warming has been associated with declines in late-stage *C. finmarchicus*, altered phenology, and reduced prey availability for higher trophic levels (Evans *et al.,* 2025).

Despite directional shifts in community weighted mean traits and functional group composition, changes in FRic and FDis with respect to species richness were largely insignificant, indicating that the volume of occupied functional space largely tracked richness-based expectations (Supplementary Fig. 1). Increases in FDis therefore reflected redistribution of biomass away from dominant large-calanoid traits toward previously less important omnivorous and recycling-associated strategies already present within the regional species pool. The persistence of non-significant ses.FRic at HL2 implies that functional redundancy remained relatively high despite gradual changes in ecosystem functioning and trophic structure (Tang *et al.,* 2022; Benedetti *et al.,* 2025). Elevated ses.FRic, particularly at P5 between 2006 and 2007, coincides with the timing of the changes in relative FG abundances and may indicate temporary weakening of dominant bloom-associated pathways under episodic environmental events.

Overall, the stronger long-term restructuring observed at HL2 compared with P5 suggests that cold-temperate outer shelf systems retaining substantial subarctic large-calanoid influence may be more sensitive to climate-driven ecosystem reorganization than already temperate tidally mixed shelf systems (Ji *et al.,* 2017; Ji *et al.,* 2022). These results also highlight the importance of scale when interpreting trait-based patterns. While global studies often report strong latitudinal gradients in FD and ecosystem functioning, local and regional systems such as HL2 and P5 may exhibit comparatively stable functional composition due to more constrained species pool and gradients (Mouillot *et al.,* 2013; Zhang *et al.,* 2021; Tang *et al.,* 2022). Regardless, even within these relatively localized systems, changes in dominant trait combinations and biomass structure reveal the sensitivity of shelf systems to significant changes in ecosystem functioning.

Use in future modelling

Representing zooplankton as one or two size-based grazing compartments is unlikely to capture the ecosystem dynamics observed on the Scotian Shelf and Bay of Fundy (Mitra, 2009). Comparisons between biogeochemical models and *in-situ* data in temperate ecosystems reveal similar seasonal patterns albeit with significantly reduced biomass (McGinty *et al.,* 2023). Our results support the growing view that a limited number of trait-defined functional groups disproportionately regulate trophic transfer and carbon cycling (Benedetti *et al.,* 2025). Large lipid-rich calanoids (FG B), strongly structured community biomass and traits linked to export potential, including body size, metabolic scaling, and C:N stoichiometry. Zooplankton are often treated as stoichiometrically homeostatic (Hébert *et al.,* 2016), yet this assumption masks meaningful variability at the community level. Changes in the phytoplankton and zooplankton C:N alter the balance between carbon assimilation, nitrogen retention, and excretion (Sterner and Elser, 2009; Sauterey and Ward, 2022). These shifts can propagate through the food web, modifying nutrient recycling rates, trophic transfer efficiency, and carbon export, altering both nitrogen regeneration pathways and the strength of the biological carbon pump (Stukel *et al.,* 2022).

These findings directly address challenges highlighted in the recent modelling literature, which identifies zooplankton grazing as one of the largest uncertainties in CMIP6 marine carbon cycle projections (Rohr *et al.,* 2023). Our results suggest that incorporating a small number of functionally distinct zooplankton compartments centered around species that comprise FG B may substantially improve regional biogeochemical models without requiring full species-level complexity.

CONCLUSION

Our analysis demonstrates that long-term changes in copepod community structure on the central Scotian Shelf (HL2) and in the Bay of Fundy (P5) reflect not simply taxonomic shifts, but also reorganization of functional trait space with important implications for ecosystem functioning. Across both regions, decreases in nutrients and increases in temperature acted as primary filters on community weighted means (CWM) of functional traits. While HL2 exhibited a progressive, nutrient-linked restructuring coupled to declining body size and C:N ratios, P5 showed stronger temperature–trait coupling with a delayed temporal response that begins ∼2010. The increase in functional dispersion points to a shift away from large, lipid-rich, export-efficient *Calanus* taxa toward smaller omnivorous or detrital feeders. These ecosystems are characterized by fewer larger sized species with low trait dispersion. Therefore, increases in trait dispersion suggest a decline in trait fitness more consistent with the mass-ratio hypothesis than with enhanced niche complementarity. This shift mirrors broader latitudinal and basin-scale gradients found elsewhere, particularly along thermal (Pata *et al.,* 2025) and productivity gradients (Benedetti *et al.,* 2025). Combined with the CWM of each PCoA axis, these results indicate a transition from a diatom–calanoid–fish pathway toward a more recycling-oriented, microbially coupled system, with implications for carbon export efficiency and trophic transfer. Ultimately, detecting and interpreting long term community shifts through functional traits, rather than taxonomy alone, provides greater insight about how environmentally driven community changes can alter overall ecosystem functioning.

ACKNOWLEDGEMENTS

Fisheries and Oceans Canada (DFO) supported Atlantic Zone Monitoring Program plankton and environmental observations, and the authors thank the DFO Science staff and vessel officers and crew who contributed to sample collection, sample analysis, and data processing and management. Benoit Casault and Chantelle Layton assisted with extraction of AZMP data for this analysis. This work was supported by the Simons Collaboration on Computational Biogeochemical Modelling of Marine Ecosystems (CBIOMES) (Grant ID: 549935 to AJI)

and NSERC Canada. We are also thankful for the comments of two anonymous reviewers that helped us make significant improvements to the final manuscript.

DATA AVAILABILITY

All data and R code used in the analysis for this paper can be found at 10.5281/zenodo.21495420.

REFERENCES

Barton, A. D., Pershing, A. J., Litchman, E., Record, N. R., Edwards, K. F., Finkel, Z. V., Kiørboe, T. and Ward, B. A. (2013) The biogeography of marine plankton traits. *Ecol. Lett.*, **16**, 522–534. https://doi.org/10.1111/ele.12063.

Beaugrand, G., Brander, K. M., Alistair Lindley, J., Souissi, S. and Reid, P. C. (2003) Plankton effect on cod recruitment in the North Sea. *Nature*, **426**, 661–664. https://doi.org/10.1038/nature02164.

Beaugrand, G., Reid, P. C., Ibanez, F., Lindley, J. A. and Edwards, M. (2002) Reorganization of North Atlantic marine copepod biodiversity and climate. *Science*, **296**, 1692–1694. https://doi.org/10.1126/science.1071329.

Becker, É. C., Macedo-Soares, L. C., Marcolin, C. R., Brandao, M. C., Stemmann, L., Mazzocchi, M. G. and Freire, A. S. (2024) Oceanographic features boost latitudinal patterns in copepod body size distribution in the South Atlantic. *Limnol. Oceanogr.*, **69**, 2668–2679. https://doi.org/10.1002/lno.12694.

Becker, É. C., Mazzocchi, M. G., de Macedo-Soares, L. C. P., Brandão, M. C. and Freire, A. S. (2021) Latitudinal gradient of copepod functional diversity in the South Atlantic Ocean. *Prog. Oceanogr.*, **199**, 102710. https://doi.org/10.1016/j.pocean.2021.102710.

Benedetti, F., Gasparini, S. and Ayata, S. D. (2016) Identifying copepod functional groups from species functional traits. *J. Plankton Res.*, **38**, 159–166. https://doi.org/10.1093/plankt/fbv096.

Benedetti, F., Vogt, M., Righetti, D., Guilhaumon, F. and Ayata, S. D. (2018) Do functional groups of planktonic copepods differ in their ecological niches? *J. Biogeogr.*, **45**, 604–616. https://doi.org/10.1111/jbi.13166.

Benedetti, F., Wydler, J., Clerc, C., Knecht, N. and Vogt, M. (2025) Emergent relationships between the functional diversity of marine planktonic copepods and ecosystem functioning in the global ocean. *Glob. Change Biol.*, **31**, e70094. https://doi.org/10.1111/gcb.70094.

Benedetti, F., Wydler, J. and Vogt, M. (2023) Copepod functional traits and groups show divergent biogeographies in the global ocean. *J. Biogeogr.*, **50**, 8–22. https://doi.org/10.1111/jbi.14512.

Brandão, M. C., Benedetti, F., Martini, S., Soviadan, Y. D., Irisson, J. O., Romagnan, J. B., Elineau, A., Desnos, C. *et al.* (2021) Macroscale patterns of oceanic zooplankton composition and size structure. *Sci. Rep.*, **11**, 15714.

Brun, P., Payne, M. R. and Kiørboe, T. (2017) A trait database for marine copepods. *Earth Syst. Sci. Data*, **9**, 99–113. https://doi.org/10.5194/essd-9-99-2017.

Brun, P., Zimmermann, N. E., Graham, C. H., Lavergne, S., Pellissier, L., Münkemüller, T. and Thuiller, W. (2019) The productivity-biodiversity relationship varies across diversity dimensions. *Nat. Commun.*, **10**, 5691. https://doi.org/10.1038/s41467-019-13678-1.

Campbell, M. D., Schoeman, D. S., Venables, W., Abu-Alhaija, R., Batten, S. D., Chiba, S., Coman, F., Davies, C. H. *et al.* (2021) Testing Bergmann's rule in marine copepods. *Ecography*, **44**, 1283–1295. https://doi.org/10.1111/ecog.05545.

Casault, B., Beazley, L., Johnson, C., Devred, E. and Head, E. (2024) *Chemical and Biological Oceanographic Conditions on the Scotian Shelf and in the Eastern Gulf of Maine during 2022*, Fisheries and Oceans Canada, Maritimes Region.

Castellani, C., Irigoien, X., Harris, R. P. and Lampitt, R. S. (2005) Feeding and egg production of Oithona similis in the North Atlantic. *Mar. Ecol. Prog. Ser.*, **288**, 173–182.

Dahms, H. U., Tseng, L. C. and Hwang, J. S. (2015) Biogeographic distribution of the cyclopoid copepod genus Oithona–from mesoscales to global scales. *J. Exp. Mar. Biol. Ecol.*, **467**, 26–32.

Deschamps, M. M., Boersma, M., Meunier, C. L., Kirstein, I. V., Wiltshire, K. H. and Di Pane, J. (2024) Major shift in the copepod functional community of the southern North Sea and potential environmental drivers. *ICES J. Mar. Sci.*, **81**, 540–552. https://doi.org/10.1093/icesjms/fsad160.

Djeghri, N., Boyé, A., Ostle, C. and Hélaouët, P. (2023) Reinterpreting two regime shifts in North Sea plankton communities through the lens of functional traits. *Glob. Ecol. Biogeogr.*, **32**, 962–975. https://doi.org/10.1111/geb.13659.

Dullaert, E. C., Runge, J. A., Karp-Boss, L., Shellito, S., Thompson, C. R. and Jones, R. J. (2026) Response of the mesozooplankton community in the western Gulf of Maine to changing oceanographic conditions: the 2010 regime shift. *J. Plankton Res.*, **48**, fbaf066.

Edwards, M., Hélaouët, P., Goberville, E., Lindley, A., Tarling, G. A., Burrows, M. T. and Atkinson, A. (2021) North Atlantic warming over six decades drives decreases in krill abundance with no associated range shift. *Commun. Biol.*, **4**, 644. https://doi.org/10.1038/s42003-021-02159-1.

Evans, T. C., Record, N. R., Ross, C. H. and Thorne, L. H. (2025) Beyond Calanus: changes to the copepod community in the Northeast USA and implications for North Atlantic right whale foraging energetics. *Endanger. Species Res.*, **56**, 1–17. https://doi.org/10.3354/esr01376.

Freer, J. J., Daase, M. and Tarling, G. A. (2022) Modelling the biogeographic boundary shift of Calanus finmarchicus reveals drivers of Arctic Atlantification by subarctic zooplankton. *Glob. Change Biol.*, **28**, 429–440.

Gallienne, C. P. and Robins, D. B. (2001) Is Oithona the most important copepod in the world's oceans? *J. Plankton Res.*, **23**, 1421–1432. https://doi.org/10.1093/plankt/23.12.1421.

Gonzalez, A., Germain, R. M., Srivastava, D. S., Filotas, E., Dee, L. E., Gravel, D., Thompson, P. L., Isbell, F. *et al.* (2020) Scaling-up biodiversity-ecosystem functioning research. *Ecol. Lett.*, **23**, 757–776. https://doi.org/10.1111/ele.13456.

Götzenberger, L., de Bello, F., Bråthen, K. A., Davison, J., Dubuis, A., Guisan, A., Lepš, J., Lindborg, R. *et al.* (2012) Ecological assembly rules in plant communities—approaches, patterns and prospects. *Biol. Rev.*, **87**, 111–127. https://doi.org/10.1111/j.1469-185X.2011.00187.x.

Greene, C. H., Meyer-Gutbrod, E., Monger, B. C., McGarry, L. P., Pershing, A. J., Belkin, I. M., Fratantoni, P. S., Mountain, D. G. *et al.* (2013) Remote climate forcing of decadal-scale regime shifts in Northwest Atlantic shelf ecosystems. *Limnol. Oceanogr.*, **58**, 803–816. https://doi.org/10.4319/lo.2013.58.3.0803.

Grime, J. P. (1998) Benefits of plant diversity to ecosystems: immediate, filter and founder effects. *J. Ecol.*, **86**, 902–910. https://doi.org/10.1046/j.1365-2745.1998.00306.x.

Head, E. J. and Pepin, P. (2010) Spatial and inter-decadal variability in plankton abundance and composition in the Northwest Atlantic (1958–2006). *J. Plankton Res.*, **32**, 1633–1648. https://doi.org/10.1093/plankt/fbq090.

Head, E. J. H., Harris, L. R. and Yashayaev, I. (2003) Distributions of Calanus spp. and other mesozooplankton in the Labrador Sea in relation to hydrography in spring and summer (1995–2000). *Prog. Oceanogr.*, **59**, 1–30. https://doi.org/10.1016/S0079-6611(03)00111-3.

Hébert, M. P., Beisner, B. E. and Maranger, R. (2016) A meta-analysis of zooplankton functional traits influencing ecosystem function. *Ecology*, **97**, 1069–1080. https://doi.org/10.1890/15-1084.1.

Hébert, M. P., Beisner, B. E. and Maranger, R. (2017) Linking zooplankton communities to ecosystem functioning: toward an effect-trait framework. *J. Plankton Res.*, **39**, 3–12. https://doi.org/10.1093/plankt/fbw068.

Helenius, L. K., Head, E. J., Jekielek, P., Orphanides, C. D., Pepin, P., Perrin, G., Plourde, S., Ringuette, M. *et al.* (2024) Spatial variability

in size and lipid content of the marine copepod Calanus finmarchicus across the Northwest Atlantic continental shelves: implications for North Atlantic right whale prey quality. *J. Plankton Res.*, **46**, 25–40. https://doi.org/10.1093/plankt/fbad047.

Heneghan, R. F., Everett, J. D., Sykes, P., Batten, S. D., Edwards, M., Takahashi, K., Suthers, I. M., Blanchard, J. L. *et al.* (2020) A functional size-spectrum model of the global marine ecosystem that resolves zooplankton composition. *Ecol. Model.*, **435**, 109265. https://doi.org/10.1016/j.ecolmodel.2020.109265.

Hooper, D. U., Chapin, F. S. III, Ewel, J. J., Hector, A., Inchausti, P., Lavorel, S., Lawton, J. H., Lodge, D. M. *et al.* (2005) Effects of biodiversity on ecosystem functioning: a consensus of current knowledge. *Ecol. Monogr.*, **75**, 3–35. https://doi.org/10.1890/04-0922.

Huggett, J. A., Noyon, M., Carstensen, J. and Walker, D. R. (2023) Patterns in the plankton–Spatial distribution and long-term variability of copepods on the Agulhas Bank. *Deep-Sea Res. II: Top. Stud. Oceanogr.*, **208**, 105265.

Johnson, C. L., Runge, J. A., Curtis, K. A., Durbin, E. G., Hare, J. A., Incze, L. S., Link, J. S., Melvin, G. D. *et al.* (2011) Biodiversity and ecosystem function in the Gulf of Maine: pattern and role of zooplankton and pelagic nekton. *PLoS One*, **6**, e16491. https://doi.org/10.1371/journal.pone.0016491.

Ji, R., Feng, Z., Jones, B. T., Thompson, C., Chen, C., Record, N. R. and Runge, J. A. (2017) Coastal amplification of supply and transport (CAST): a new hypothesis about the persistence of Calanus finmarchicus in the Gulf of Maine. *ICES J. Mar. Sci.*, **74**, 1865–1874.

Ji, R., Runge, J. A., Davis, C. S. and Wiebe, P. H. (2022) Drivers of variability of Calanus finmarchicus in the Gulf of Maine: roles of internal production and external exchange. *ICES J. Mar. Sci.*, **79**, 775–784.

Jónasdóttir, S. H., Visser, A. W., Richardson, K. and Heath, M. R. (2015) Seasonal copepod lipid pump promotes carbon sequestration in the deep North Atlantic. *Proc. Natl. Acad. Sci. U. S. A.*, **112**, 12122–12126. https://doi.org/10.1073/pnas.1512110112.

Kiørboe, T. (2011) How zooplankton feed: mechanisms, traits and trade-offs. *Biol. Rev.*, **86**, 311–339. https://doi.org/10.1111/j.1469-185X.2010.00148.x.

Lehmann, N., Reed, D. C., Buchwald, C., Lavoie, D., Yeats, P. A., Mei, Z. P., Wang, Z. and Johnson, C. L. (2023) Decadal variability in subsurface nutrient availability on the Scotian shelf reflects changes in the Northwest Atlantic Ocean. *J. Geophys. Res. Oceans*, **128**, e2023JC019928. https://doi.org/10.1029/2023JC019928.

Lenz, P. H. (2012) The biogeography and ecology of myelin in marine copepods. *J. Plankton Res.*, **34**, 575–589.

Litchman, E., Ohman, M. D. and Kiørboe, T. (2013) Trait-based approaches to zooplankton communities. *J. Plankton Res.*, **35**, 473–484. https://doi.org/10.1093/plankt/fbt019.

McCann, K. S. (2000) The diversity–stability debate. *Nature*, **405**, 228–233. https://doi.org/10.1038/35012234.

McGinty, N., Barton, A. D., Record, N. R., Finkel, Z. V. and Irwin, A. J. (2018) Traits structure copepod niches in the North Atlantic and Southern Ocean. *Mar. Ecol. Prog. Ser.*, **601**, 109–126. https://doi.org/10.3354/meps12660.

McGinty, N., Irwin, A. J., Finkel, Z. V. and Dutkiewicz, S. (2023) Using ecological partitions to assess zooplankton biogeography and seasonality. *Front. Mar. Sci.*, **10**, 989770. https://doi.org/10.3389/fmars.2023.989770.

Melle, W., Runge, J. A., Head, E., Plourde, S., Castellani, C., Licandro, P., Pierson, J., Jónasdóttir, S. H. *et al.* (2015) Biogeography of key mesozooplankton species in the North Atlantic and egg production of Calanus finmarchicus. *Earth Syst. Sci. Data*, **7**, 223–230. https://doi.org/10.5194/essd-7-223-2015.

Meyer-Gutbrod, E. L., Greene, C. H., Davies, K. T. and Johns, D.G. (2021) Ocean regime shift is driving collapse of the North Atlantic right whale population. *Oceanography*, **34**, 22–31.

Mitchell, M. R., Harrison, G., Pauley, K., Gagné, A., Maillet, G. and Strain, P. (2002) *Atlantic Zonal Monitoring Program Sampling Protocol (p. 23)*, Fisheries & Oceans Canada, Maritimes Region, Ocean Sciences Division, Bedford Institute of Oceanography.

Mitra, A. (2009) Are closure terms appropriate or necessary descriptors of zooplankton loss in nutrient–phytoplankton–zooplankton type models? *Ecol. Model.*, **220**, 611–620. https://doi.org/10.1016/j.ecolmodel.2008.12.008.

Møller, E. F. (2007) Production of dissolved organic carbon by sloppy feeding in the copepods Acartia tonsa, Centropages typicus, and Temora longicornis. *Limnol. Oceanogr.*, **52**, 79–84.

Morán, X. A. G., Gasol, J. M., Pernice, M. C., Mangot, J. F., Massana, R., Lara, E., Vaqué, D. and Duarte, C. M. (2017) Temperature regulation of marine heterotrophic prokaryotes increases latitudinally as a breach between bottom-up and top-down controls. *Glob. Change Biol.*, **23**, 3956–3964. https://doi.org/10.1111/gcb.13730.

Moritz, S. and Bartz-Beielstein, T. (2017) imputeTS: time series missing value imputation in R. *The R Journal*, **9**, 207–218. https://doi.org/10.32614/RJ-2017-009.

Mouillot, D., Graham, N. A., Villéger, S., Mason, N. W. and Bellwood, D. R. (2013) A functional approach reveals community responses to disturbances. *Trends Ecol. Evol.*, **28**, 167–177. https://doi.org/10.1016/j.tree.2012.10.004.

Mouillot, D., Loiseau, N., Grenié, M., Algar, A. C., Allegra, M., Cadotte, M. W., Casajus, N., Denelle, P.S *et al.* (2021) The dimensionality and structure of species trait spaces. *Ecol. Lett.*, **24**, 1988–2009. https://doi.org/10.1111/ele.13778.

Pata, P. R., Galbraith, M., Young, K., Sastri, A. R., Perry, R. I. and Hunt, B. P. (2025) Functional characteristics of zooplankton bioregions along the cross-shelf gradient. *Prog. Oceanogr.*, **238**, 103559. https://doi.org/10.1016/j.pocean.2025.103559.

Pata, P. R. and Hunt, B. P. (2025) Harmonizing marine zooplankton trait data toward a mechanistic understanding of ecosystem functioning. *Limnol. Oceanogr.*, **70**, S8–S27. https://doi.org/10.1002/lno.12478.

Pepin, P., Johnson, C. L., Harvey, M., Casault, B., Chassé, J., Colbourne, E. B., Galbraith, P. S., Hebert, D. *et al.* (2015) A multivariate evaluation of environmental effects on zooplankton community structure in the western North Atlantic. *Prog. Oceanogr.*, **134**, 197–220. https://doi.org/10.1016/j.pocean.2015.01.017.

Pershing, A. J., Alexander, M. A., Hernandez, C. M., Kerr, L. A., Le Bris, A., Mills, K. E., Nye, J. A., Record, N. R. *et al.* (2015) Slow adaptation in the face of rapid warming leads to collapse of the Gulf of Maine cod fishery. *Science*, **350**, 809–812. https://doi.org/10.1126/science.aac9819.

Pershing, A. J., Alexander, M. A., Brady, D. C., Brickman, D., Curchitser, E. N., Diamond, A. W., McClenachan, L., Mills, K. E. *et al.* (2021) Climate impacts on the Gulf of Maine ecosystem: a review of observed and expected changes in 2050 from rising temperatures. *Elem. Sci. Anth.*, **9**, 00076.

Pershing, A. J. and Kemberling, A. (2024) Decadal comparisons identify the drivers of persistent changes in the zooplankton community structure in the northwest Atlantic. *ICES J. Mar. Sci.*, **81**, 564–574.

Pomerleau, C., Sastri, A. R. and Beisner, B. E. (2015) Evaluation of functional trait diversity for marine zooplankton communities in the northeast subarctic Pacific Ocean. *J. Plankton Res.*, **37**, 712–726. https://doi.org/10.1093/plankt/fbv045.

Pomeroy, L. R., le B, W. P. J., Azam, F. and Hobbie, J. E. (2007) The microbial loop. *Oceanography*, **20**, 28–33. https://doi.org/10.5670/oceanog.2007.45.

Prowe, A. F., Visser, A. W., Andersen, K. H., Chiba, S. and Kiørboe, T. (2019) Biogeography of zooplankton feeding strategy. *Limnol. Oceanogr.*, **64**, 661–678. https://doi.org/10.1002/lno.11067.

Record, N. R., Ji, R., Maps, F., Varpe, Ø., Runge, J. A., Petrik, C. M. and Johns, D. (2018) Copepod diapause and the biogeography of the marine lipidscape. *J. Biogeogr.*, **45**, 2238–2251. https://doi.org/10.1111/jbi.13414.

Record, N. R., Runge, J. A., Pendleton, D. E., Balch, W. M., Davies, K. T., Pershing, A. J., Johnson, C. L., Stamieszkin, K. *et al.* (2019) Rapid climate-driven circulation changes threaten conservation of endangered North Atlantic right whales. *Oceanography*, **32**, 162–169. https://doi.org/10.5670/oceanog.2019.201.

Rohr, T., Richardson, A. J., Lenton, A., Chamberlain, M. A. and Shadwick, E. H. (2023) Zooplankton grazing is the largest source of uncertainty

for marine carbon cycling in CMIP6 models. *Commun. Earth Environ.*, **4**, 212. https://doi.org/10.1038/s43247-023-00871-w.

Runge, J. A., Thompson, C. R., Shellito, S., Dullaert, E. C., Honda, I. A., Vandemark, D., Pugh, D., Young-Morse, R. *et al.* (2025) Zooplankton monitoring at fixed station time series records responses of the foundation species, Calanus finmarchicus, to seasonal and multiannual drivers in the western Gulf of Maine. *ICES J. Mar. Sci.*, **82**, fsaf037.

Saba, G. K., Steinberg, D. K. and Bronk, D. A. (2009) Effects of diet on release of dissolved organic and inorganic nutrients by the copepod Acartia tonsa. *Mar. Ecol. Prog. Ser.*, **386**, 147–161.

Sameoto, D., Neilson, J. and Waldron, D. (1994) Zooplankton prey selection by juvenile fish in Nova Scotian shelf basins. *J. Plankton Res.*, **16**, 1003–1019. https://doi.org/10.1093/plankt/16.8.1003.

Sauterey, B. and Ward, B. A. (2022) Environmental control of marine phytoplankton stoichiometry in the North Atlantic Ocean. *Proc. Natl. Acad. Sci. U. S. A.*, **119**, e2114602118. https://doi.org/10.1073/pnas.2114602118.

Severo, A., Becker, É. C., Acha, E. M., Segura, V. and Cepeda, G. D. (2026) Zooplankton functional and taxonomic diversity: linking functional traits and springtime environmental gradients at the Patagonian shelf-break front. *Prog. Oceanogr.*, **244**, 103728. https://doi.org/10.1016/j.pocean.2026.103728.

Sorochan, K. A., Plourde, S., Morse, R., Pepin, P., Runge, J., Thompson, C. and Johnson, C. L. (2019) North Atlantic right whale (*Eubalaena glacialis*) and its food: (II) interannual variations in biomass of Calanus spp. on western North Atlantic shelves. *J. Plankton Res.*, **41**, 687–708. https://doi.org/10.1093/plankt/fbz044.

Steinberg, D. K. and Landry, M. R. (2017) Zooplankton and the ocean carbon cycle. *Annu. Rev. Mar. Sci.*, **9**, 413–444. https://doi.org/10.1146/annurev-marine-010814-015924.

Steinberg, D. K., Ruck, K. E., Gleiber, M. R., Garzio, L. M., Cope, J. S., Bernard, K. S., Stammerjohn, S. E., Schofield, O. M. *et al.* (2015) Long-term (1993–2013) changes in macrozooplankton off the Western Antarctic Peninsula. *Deep-Sea Res. I Oceanogr. Res. Pap.*, **101**, 54–70. https://doi.org/10.1016/j.dsr.2015.02.009.

Sterner, R. W. and Elser, J. J. (2009) Ecological stoichiometry. *The Princeton guide to ecology*, 376–385. https://doi.org/10.1515/9781400833023.376.

Stukel, M. R., Décima, M. and Landry, M. R. (2022) Quantifying biological carbon pump pathways with a data-constrained mechanistic model ensemble approach. *Biogeosciences*, **19**, 3595–3624. https://doi.org/10.5194/bg-19-3595-2022.

Tang, Q., Yang, J. and Sun, D. (2022) Functional diversity of copepod assemblages along a basin-scale latitudinal gradient in the North Pacific Ocean. *Ecol. Indic.*, **141**, 109112. https://doi.org/10.1016/j.ecolind.2022.109112.

Therriault, J. C., Petrie, B., Pepin, P., Gagnon, J., Gregory, D., Helbig, J., Herman, A., Lefaivre, D. *et al.* (2002) *The Atlantic Zone Monitoring Program after 5 Years: A Focal Point for Monitoring the Marine Environment of the East Coast*.

Turner, J. T. (2015) Zooplankton fecal pellets, marine snow, phytodetritus and the ocean's biological pump. *Prog. Oceanogr.*, **130**, 205–248. https://doi.org/10.1016/j.pocean.2014.08.005.

Wiebe, P. H., Baumgartner, M. F., Copley, N. J., Lawson, G. L., Davis, C., Ji, R. and Greene, C. H. (2022) Does predation control the diapausing stock of Calanus finmarchicus in the Gulf of Maine? *Prog. Oceanogr.*, **206**, 102861.

Zhang, Z., Zhuang, Y., Chen, H., Lu, S., Li, Y., Ge, R., Chen, C. and Liu, G. (2021) Effects of Prorocentrum donghaiense bloom on zooplankton functional groups in the coastal waters of the East China Sea. *Mar. Pollut. Bull.*, **172**, 112878.

Journal of Plankton Research, 2026, Vol. 48, No. 5, fbag065
https://doi.org/10.1093/plankt/fbag065
Original Article